Functional Self-Assembly of Hydrogen-Bonded Networks. Construction of Aromatic Stacks and Columns and Cavity-Size Control via Flexible Intercalation of 1D Chains Having Orthogonal Aromatic Substituents

Ken Endo,[†] Takayoshi Ezuhara,[†] Masayuki Koyanagi,[†] Hideki Masuda,[‡] and Yasuhiro Aoyama*,[†]

Contribution from the Institute for Fundamental Research of Organic Chemistry, Kyushu University, Hakozaki, Higashi-Ku, Fukuoka 812-81, Japan, and Department of Applied Chemistry, Nagoya Institute of Technology, Gokiso-Cho, Showa-Ku, Nogoya 466, Japan

Received January 26, 1996. Revised Manuscript Received October 30, 1996[⊗]

Abstract: Anthracene−monoresorcinol derivative **1** forms hydrogen-bonded poly(resorcinol) 1D chains, which self-assemble via interpenetration or intercalation of the orthogonal anthracene (A) *substituents*. Guest-binding in the resulting cavities leads to either, depending on the guests (G, aromatic or aliphatic), an alternate ···A·G·A·G··· (*monomeric*) or an ···A·A·G·G··· (*dimeric*) lattice pattern. The monomeric lattices show a remarkable linear-alkyl vs branched-alkyl selectivity in the guest-binding. The dimeric lattices are characterized by their exclusive emission of excimer fluorescence. Self-assembly of the present 1D chains is thus functional and also flexible and dynamic; removal, addition, and exchange of guest molecules readily occur in the solid states.

Introduction

Design of crystal structures is a rapidly growing area.[1] Many researchers take advantage of hydrogen-bonded networks to restrict relative orientation of molecules in crystals.[2] Apparently, higher-dimensional networks (3D > 2D > 1D) would be more suited for this purpose. The resulting networks further self-assemble. The design of crystal structures should therefore pay attention not only to the dimensionality and topology of the networks but also to the self-assembly thereof. Actually, however, the modes of self-assembly are still difficult to predict in many cases, as in the multifold interpenetration of higher-dimensional networks.[3]

The present work is concerned with self-assembling properties of 1D chains. We have studied the crystal structures, guest-binding properties, and fluorescence behaviors of various adducts of anthracene−monoresorcinol derivative **1** (Scheme 1) in reference to those of the corresponding 2D counterpart, i.e., anthracene−bisresorcinol compound **2** (Scheme 1).[4] We report here that the hydrogen-bonded poly(resorcinol) 1D chains *functionally* self-assemble via guest-dependent *intercalation* of the orthogonal anthracene *substituents*. This affords closely-packed aromatic stacks and columns with various photophysical properties and compact guest-binding cavities which exhibit novel thickness and chain-length selectivities.

Scheme 1

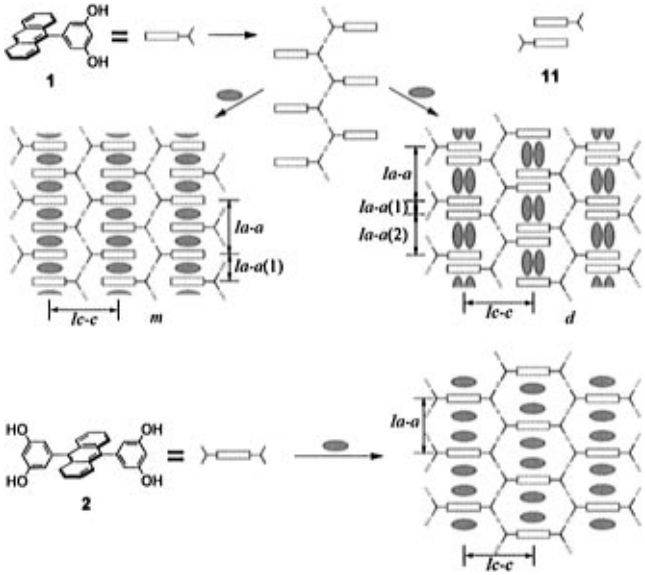

Results and Discussion

Lattice Patterns. Compound **1** (host) affords 1:1 cocrystals with a variety of guests such as esters and ketones. The host forms hydrogen-bonded (O−H···O−H) poly(resorcinol) chains, which are held together via self-intercalation of the orthogonal anthracene (A) substituents. There are two lattice patterns, *monomeric (m)* and *dimeric (d)*. In the former, two neighboring chains are symmetrically self-assembled. One molecule of the guest (G) is horizontally incorporated along the long axis of the anthracene ring in each cavity left via host−guest hydrogen-bonding (O−H···O−H···O═C). This gives an alternate ···A·G·A·G··· arrangement. In the latter the A moieties from

[†] Kyushu University.
[‡] Nagoya Institute of Technology.
[⊗] Abstract published in *Advance ACS Abstracts,* January 1, 1997.

(1) Desiraju, G. R. Crystal Engineering: *The Design of Organic Solids*; Elsevier: New York, 1989.
(2) For an excellent recent review, see: MacDonald, J. C.; Whitesides, G. M. *Chem. Rev.* **1994**, *94*, 2383−2420.
(3) (a) See, for example: (a) Ermer, O. *J. Am. Chem. Soc.* **1988**, *110*, 3747−3754. (b) Simard, M.; Su, D.; Wuest, J. D. *Ibid.* **1991**, *113*, 4696−4698. (c) Copp, S. B.; Subramanian, S.; Zaworotko, M. J. *Ibid.* **1992**, *114*, 8719−8720. (d) Reddy, D. S.; Craig, D. C.; Rae, A. D.; Desiraju, G. R. *J. Chem. Soc., Chem. Commun.* **1993**, 1737−1739. (e) Zaworotko, M. J. *Chem. Soc. Rev.* **1994**, *23*, 283−288. (f) Batten, S. R.; Hoskins, B. F.; Robson, R. *J. Am. Chem. Soc.* **1995**, *117*, 5385−5386. (g) Fujita, M.; Kwon, Y. J.; Sasaki, O.; Yamaguchi, K.; Ogura, K. *Ibid.* **1995**, *117*, 7287−7288.
(4) (a) Aoyama, Y.; Endo, K.; Kobayashi, K.; Masuda, H. *Supramol. Chem.* **1995**, *4*, 229−241. (b) Endo, K.; Sawaki, T.; Koyanagi, M.; Kobayashi, K.; Masuda, H.; Aoyama, Y. *J. Am. Chem. Soc.* **1995**, *117*, 8341−8352. (c) Aoyama, Y.; Endo, K.; Anzai, T.; Yamaguchi, Y.; Sawaki, T.; Kobayashi, K.; Kanehisa, N.; Hashimoto, H.; Kai, Y.; Masuda, H. *J. Am. Chem. Soc.* **1996**, *118*, 5562−5571.

S0002-7863(96)00292-2 CCC: $14.00

Chart 1

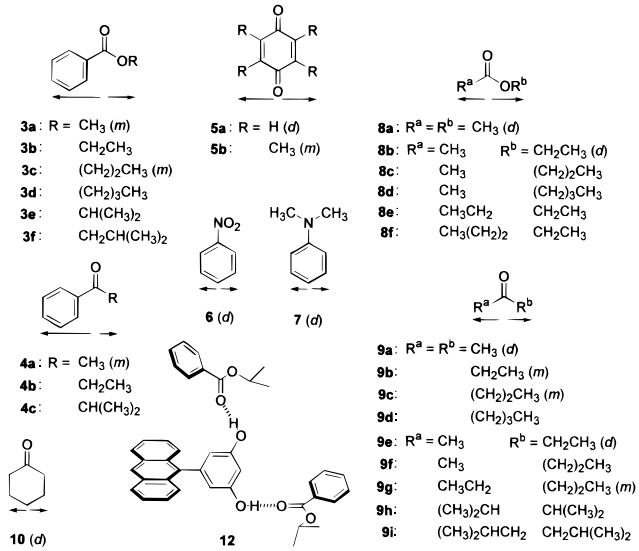

neighboring chains form face-to-face stack dimers (A·A). This mode of self-assembly affords larger cavities, in which two guest molecules are vertically bound. The two patterns *m* and *d* are schematically shown in Scheme 1, where and hereafter the anthracene and resorcinol rings are shown in red and black, respectively, guest molecules are in green, and hydrogen bonds are represented in light blue; host−guest hydrogen bonds are not shown for clarity.

In Chart 1 are shown the guest molecules **3**−**10** together with lattice patterns (*m* or *d*) for those whose crystal structures have been determined. Aromatic guests such as alkyl benzoates **3a** and **3c**, acetophenone (**4a**), and duroquinone (**5b**) give rise to pattern *m*, while benzoquinone (**5a**), nitrobenzene (**6**), and *N*,*N*-dimethylaniline (**7**) lead to pattern *d*. Quinone guests **5a** and **5b** are hydrogen-bonded to the host only at one of two C═O groups. Aliphatic esters and ketones such as methyl acetate (**8a**), ethyl acetate (**8b**), acetone (**9a**), 2-butanone (**9e**), and cyclohexanone (**10**) give adducts with pattern *d*, while 3-pentanone (**9b**) and higher homologs **9c** and **9g** result in pattern *m*. The structures of all the adducts were refined with $R < 0.09$ (Table 1), although disorder is evident for some guest molecules.[5] Except for the quinone adducts **1**·**5a** and **1**·**5b** (dark red) and nitrobenzene adduct **1**·**6** (orange),[6] all the pattern-*m* adducts are colorless and most of the pattern-*d* adducts are yellow.

The crystal structures for the duroquinone and cyclohexanone adducts **1**·**5b** and **1**·**10** as typical examples of patterns *m* and *d* are represented in parts a and b, respectively, in Figure 1, where side views of a molecular sheet (Scheme 1) and top views of two neighboring sheets are shown in stereo. The corresponding side views for the propyl benzoate, benzoquinone, ethyl acetate, and 4-heptanone adducts **1**·**3c**, **1**·**5a**, **1**·**8b**, and **1**·**9c** as other representative cases are shown in Figure 2. Those for other adducts are included in Figures I and II (Supporting Information).[7] In Table 1 are summarized the crystal data together with characteristic distances and angles.

Steric Control of Aromatic Stacks and Columns. Apparently, smaller guests (quinone **5a** vs **5b** and ketones **9a** and **9e** vs **9b**, **9c**, and **9g**) tend to prefer pattern *d*. A closer look at the structures reveals a more general rule. This is with respect to the elongation or width of apolar moieties in the direction perpendicular to the hydrogen-bonding site, as shown by arrows for the guests in Chart 1. Both R^1 and R^2 in all the pattern-*m* guests (R^1R^2C═O) except for acetophenone (**4a**) (vide infra) are at least two atoms long. On the other hand, at least one of them, i.e., R^1, in all the pattern-*d* guests has a C_1-elongation; it is either methyl (**8a**, **8b**, **9a**, and **9e**) or tied back into a six-membered ring (**5a**, **6**, **7**, and **10**). The interplane distance (face-to-face) for the anthracene stacks is $Ia-a(1) = 3.5-3.7$ Å (Table 1). Since an aromatic (anthracene) ring is ∼3.5 Å thick, this indicates that the two anthracene rings in a stack are almost in contact, as shown by a space-filling model for adduct **1**·**10** in Figure 3b. It is also a common feature of the pattern-*d* lattices that the anthracene and the resorcinol rings in compound **1** are not orthogonal with a dihedral angle (ϕ) mostly in the range of 70−80° (Table 1).

In the pattern-*m* lattices (referring to Scheme 1, Figures 1 and 2a,d, and Table 1), the anthracene and resorcinol rings are nearly orthogonal ($\phi \cong 90°$). The interplane distance (center-to-center) for the adjacent anthracene moieties is $Ia-a(1) = 7.1-7.3$ Å. The effective height or thickness of the resulting guest-binding cavities would be in the neighborhood of $7.2 - 3.5 = 3.7$ Å, which is nearly the π-electron thickness (3.5 Å) of an aromatic ring. Figure 3a shows a space-filling model for the closely packed anthracene−duroquinone alternate column in the duroquinone adduct **1**·**5b**. π-Stacking or charge-transfer interactions between anthracene and quinone rings possibly contribute to the stability of the present column. This may also explain why acetophenone (**4a**) having a methyl group forms a pattern-*m* lattice. However, it should be emphasized here again that the lattice patterns are primarily governed by steric factors and not by electronic ones. Thus, not only aromatic esters and ketones **3a**, **3c**, and **4a** as weak acceptors but also aliphatic guests **9b**, **9c**, and **9g** give rise to alternate columns in pattern *m*. Furthermore, benzoquinone (**5a**) and nitrobenzene (**6**) as strong acceptors are vertically incorporated in pattern *d*.[6]

Network Dimensionality. The general crystal structure for the 1:2 adduct **2**·2(guest)[4] of the anthracene−bisresorcinol derivative **2** is shown in Scheme 1; the actual structure of the isobutyl benzoate adduct **2**·2(**3f**) is presented in Figure III (Supporting Information). The 2D network shown is closely related to the pseudo-2D network described above. In fact, adducts **2**·2(guest) and **1**·guest are similar to each other in respect not only to the general chain/sheet/layer structures and guest-binding modes but also to the interplane distances (*Ia*−*a*) along a chain as well as intercolumn (*Ic*−*c*) and intersheet (*Is*−*s*) distances.[8] As far as hydrogen-bonding sites are concerned, 2D host **2** is equivalent to a dimer of 1D host **1**, schematically shown as structure **11** in Scheme 1. Monoanthracenyl and dianthracenyl tetraols **2** and **11** then behave similarly to form 2D and pseudo-2D hydrogen-bonded networks, respectively, but with different packing states in the resulting anthracene columns.

(5) Nonsymmetric pattern-*m* guests such as **3a**, **3c**, and **4a** are enclathrated in two phases, $R^1(C═O)R^2$ and $R^2(C═O)R^1$, which are mirror images with each other with respect to the long axis of the anthracene ring. In some cases as in **3a**, different phases lead to different hydrogen-bond distances (Table 1). *N*,*N*-Dimethylaniline (**7**) exhibits another type of disorder. Although the nitrogen atom and three carbon atoms attached to it are located, the benzene ring cannot be fixed (Figure Id in the Supporting Information). It must be rapidly swinging.

(6) As is suggested by the crystal structure, adduct **1**·**5b** is an anthracene−duroquinone charge-transfer crystal. Adducts **1**·**5a** and **1**·**6**, on the other hand, may be resorcinol−benzoquinone and resorcinol−nitrobenzene charge-transfer crystals, respectively. The guest molecules **5a** and **6** are perpendicular to the anthracene moieties but are in a partial overlap with resorcinol rings in adjacent sheets. They are roughly parallel with a spacing of ∼3.8 Å.

(7) For the complicated crystal structure of adduct **1**·**6**, see footnote *c* of Table 1.

(8) For adduct **2**·2(**3a**), $Ia-a = 13.40$ (center-to-center), $Ic-c = 10.20$, and $Is-s = 6.20$.[4a] For adduct **2**·2(**3c**), they are 13.70, 9.93, and 7.16, respectively.[4a] These distances may be compared with those for adducts **1**·**3a** and **1**·**3c** shown in Table 1; the interplane distance along a chain is $Ia-a = 2(Ia-a(1)) = 14.26$ and 14.56 for adducts **1**·**3a** and **1**·**3c**, respectively (cf. footnote *b* of Table 1).

Table 1. Crystallographic Data and Characteristic Distances and Angles for Various Adducts **1**·Guest[a]

	3a (*m*)	**3c** (*m*)	**4a** (*m*)	**5b** (*m*)	**9b** (*m*)	**9c** (*m*)	**9g** (*m*)	**5a** (*d*)	**6**[c] (*d*)	**7** (*d*)	**8a** (*d*)	**8b** (*d*)	**9a** (*d*)	**9e** (*d*)	**10** (*d*)
formula	$C_{28}H_{22}O_4$	$C_{30}H_{26}O_4$	$C_{28}H_{22}O_3$	$C_{30}H_{26}O_4$	$C_{25}H_{24}O_3$	$C_{27}H_{28}O_3$	$C_{26}H_{26}O_3$	$C_{26}H_{18}O_4$	$C_{78}H_{57}O_{12}N_3$	$C_{28}H_{25}O_2N$	$C_{23}H_{20}O_4$	$C_{24}H_{22}O_4$	$C_{23}H_{20}O_3$	$C_{24}H_{22}O_3$	$C_{26}H_{24}O_3$
formula weight	422.48	450.53	406.48	450.53	372.46	400.52	386.49	394.43	1228.32	407.51	360.41	374.44	344.41	358.44	384.47
crystal system	monoclinic	orthorhombic	orthorhombic	monoclinic	monoclinic	monoclinic	monoclinic	monoclinic	monoclinic	monoclinic	monoclinic	monoclinic	monoclinic	monoclinic	monoclinic
space group	$P2_1/n$	*Pnma*	*Pnma*	*Cc*	$P2_1/n$	$P2_1/a$	$P2_1/a$	$P2_1/n$	$P2_1/a$	$P2_1/c$	$P2_1/c$	$P2_1/c$	$P2_1/c$	$P2_1/c$	$P2_1/n$
color	colorless	colorless	colorless	dark-red	colorless	colorless	colorless	dark-red	orange	yellow	yellow	yellow	colorless	yellow	colorless
a, Å	10.845(4)	14.567(2)	13.981(2)	14.542(1)	10.629(5)	14.564(1)	14.417(2)	9.022(3)	20.880(3)	9.371(2)	9.1596(7)	9.123(1)	9.136(2)	9.147(2)	8.792(2)
b, Å	14.265(2)	15.160(3)	14.276(3)	11.640(1)	14.302(2)	10.712(3)	10.649(4)	13.757(3)	13.874(3)	13.795(1)	13.7338(9)	13.870(3)	13.585(2)	13.765(1)	13.9258(9)
c, Å	13.967(2)	10.752(2)	10.853(4)	14.299(1)	13.970(2)	15.115(2)	14.856(2)	16.630(3)	21.705(4)	14.918(2)	16.0198(6)	16.504(1)	15.816(2)	16.250(2)	17.223(1)
β, deg	90.14(2)			105.063(6)	91.80(2)	107.140(8)	106.78(1)	104.06(2)	93.72(1)	106.45(1)	104.879(4)	104.365(8)	104.56(1)	105.16(1)	101.101(10)
V, Å^3	2160.8(7)	2374.4(7)	2166.2(8)	2337.3(3)	2122(1)	2253.2(6)	2183.7(8)	2002.2(8)	6274(1)	1849.6(5)	1947.7(2)	2023.0(4)	1899.8(5)	1974.7(5)	2069.1(5)
Z	4	4	4	4	4	4	4	4	4	4	4	4	4	4	4
R	0.073	0.083	0.088	0.040	0.061	0.055	0.055	0.040	0.043	0.058	0.052	0.055	0.051	0.048	0.085
GOF	1.75	3.34	4.05	1.28	1.48	1.33	1.24	1.23	1.51	1.38	1.28	1.23	1.33	1.25	1.55
Ia−*a*(1),[b] Å	7.13	7.28	7.14	7.15	7.15	7.28	7.21	3.60	*c*	3.53	3.64	3.69	3.65	3.70	3.69
Ia−*a*(2),[b] Å								9.90	*c*	9.74	9.66	9.81	9.36	9.57	9.67
Ic−*c*, Å	10.85	10.75	10.85	11.64	10.63	10.71	10.65	10.38	10.40	10.19	10.51	10.68	10.47	10.53	10.40
Is−*s*, Å	6.98	7.58	6.99	7.02	6.98	7.22	7.11	7.01	7.13	6.58	6.75	6.83	6.68	6.82	7.15
Io−*o*(H−H), Å	2.81	2.93	2.78	2.85	2.84	2.82	2.79	2.74	*c*	2.93	2.80	2.83	2.75	2.76	2.74
Io−*o*(H−G), Å	2.75, 2.82	2.71	2.76	2.72	2.66	2.62	2.63, 2.67	2.73	*c*	3.13[d]	2.70	2.71	2.68	2.68	2.64
ϕ, deg	88.74	90.00	90.00	85.83	87.35	88.00	89.96	68.56	*c*	82.51	80.70	79.60	79.80	78.23	72.27

[a] The boldface compound number in the column heads is the guest, and the italic letter is the lattice pattern. *Ia*−*a*, *Ic*−*c*, and *Is*−*s* are interplane, intercolumn, and intersheet distances, respectively, in reference to Scheme 1 and Figure 1. *Io*−*o*(H−H) and *Io*−*o*(H−G) are host−host and host−guest hydrogen-bond distances. ϕ is the dihedral angle between the anthracene and resorcinol rings in compound **1**. [b] The interplane distances (*Ia*−*a*(1) and *Ia*−*a*(2)) in pattern-*d* adducts are the face-to-face distances for the adjacent anthracene rings. Those (*Ia*−*a*(1)) in pattern-*m* adducts, where adjacent anthracene rings are not parallel, are *Ia*−*a*(1) = 0.5(*Ia*−*a*); *Ia*−*a* is the center-to-center distance for the anthracene moieties along a chain (Scheme 1). [c] Adduct **1**·**6** has a complicated crystal structure consisting of two different sheets (s and s′) which are layered into ···s·s′·s′·s·s′·s′···: *Ia*−*a*(1) = 3.63, 3.66; *Ia*−*a*(2) = 9.12, 9.62. One sheet is composed of two independent molecules of both host and guest, while in the other all the host and guest molecules are equivalent. As a consequence, there are three crystallographically nonequivalent molecules of both host and guest: *Io*−*o*(H−H) = 2.75, 2.77, 2.79; *Io*−*o*(H−G) = 2.96, 2.98, 3.07; ϕ = 77.09, 79.31, 86.28. Side views of two different sheets are shown in Figures Ic and Ic′ (Supporting Information). [d] O−N distance.

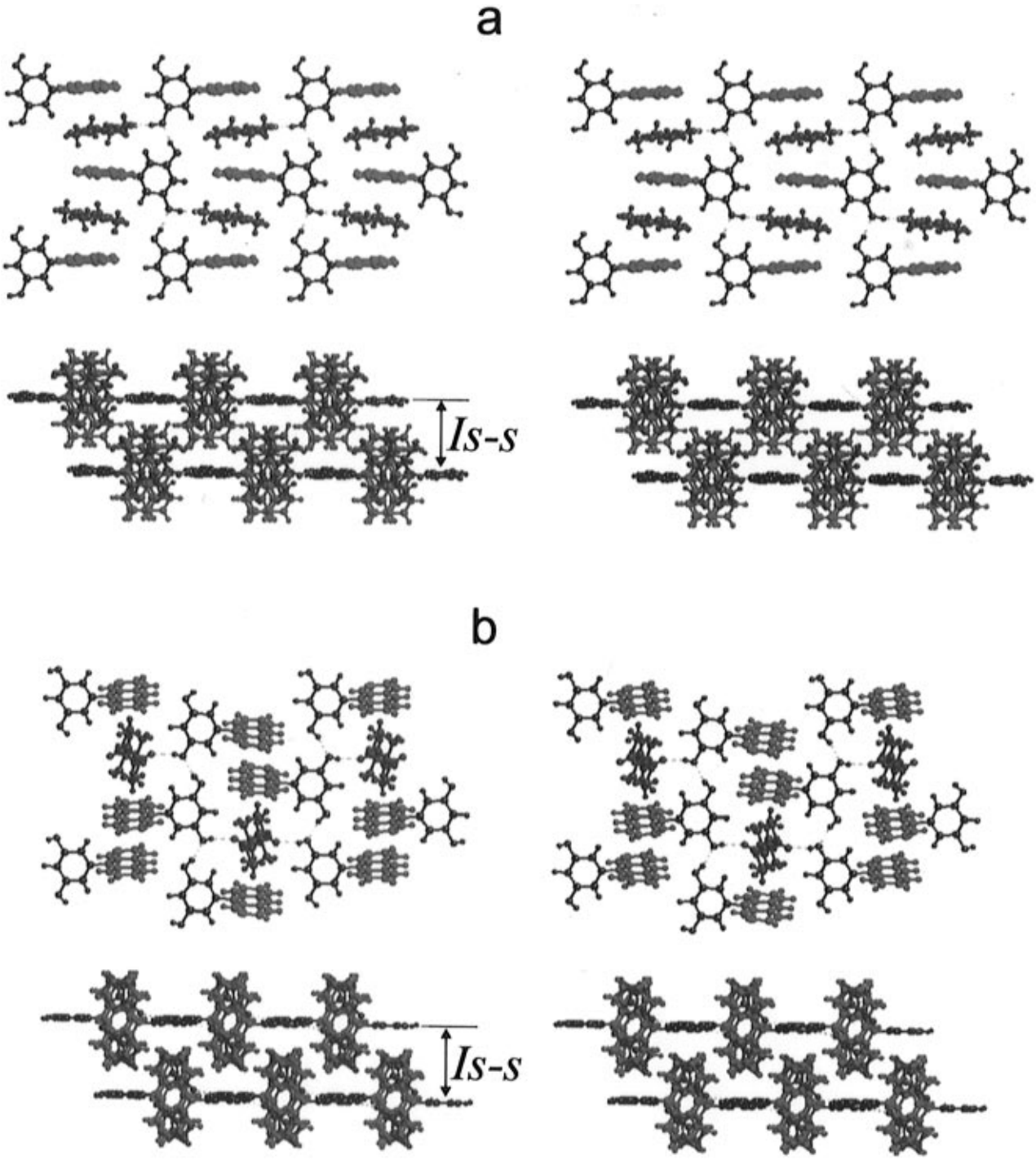

Figure 1. Crystal structures of adduct **1·5b** (a) and **1·10** (b) in stereo; side view of a molecular sheet (top) and top view of two adjacent sheets (bottom). Anthracene and resorcinol rings are in red and black, respectively, guest molecules are in green, and hydrogen bonds are in light blue.

Fluorescence Behaviors. The fluorescence behaviors of the adducts in the solid state depend on both lattice patterns and included guest molecules.[9] Figure 4 shows typical spectra at 25 °C for adducts **1·3c** (*m*), **1·8b** (*d*), and **1·9c** (*m*). Pattern-*m* adducts except for **1·5b** emit monomer fluorescence with characteristic vibrational fine structures from the isolated anthracene (A) moieties in the range 410−440 nm.[10]

Pattern-*d* adducts with aliphatic guests emit featureless and highly red-shifted fluorescence at 509 (guest = **8a**), 506 (**8b**), 485 (**9a**), 500 (**9e**), or 459 (**10**) nm. The characteristic feature is readily understood in terms of excimer (excited dimer; (A·A)*) fluorescence[11,12] from the dimeric face-to-face anthracene stacks. Pattern-*d* adducts with aromatic guests show a diversity in their behaviors for the reasons which remain to be explored. *N*,*N*-Dimethylaniline and nitrobenzene adducts **1·7** (yellow) and **1·6** (orange)[6] show featureless fluorescence at 500 and 436 nm, respectively. On the other hand, benzoquinone adduct **1·5a** (dark red)[6] as well as duroquinone adduct **1·5b** (dark red)[6] in lattice pattern *m* are rendered nonfluorescent presumably because of electron-transfer (A* to the guest quinone) fluorescence-quenching.

(9) For a general reference on electronic spectroscopy of organic crystals, see: Pope, M.; Swenberg, C. E. *Annu. Rev. Phys. Chem.* **1984**, *35*, 613−655.

(10) Fluorescence maxima (nm) for other pattern-*m* adducts and solid anthracene are 420, 442, 465 (sh), and 500 (sh) (for **1·3a**), 414, 438, 460, and 490 (sh) (**1·9b**), 414, 437, 460, and 490 (sh) (**1·9g**), and 422, 444, 470, 493 (sh) (solid anthracene) (sh = shoulder).

(11) Chandross, E. A.; Ferguson, J. *J. Chem. Phys.* **1966**, *45*, 3564−3567.

(12) Chandross, E. A. *J. Chem. Phys.* **1965**, *43*, 4175−4176.

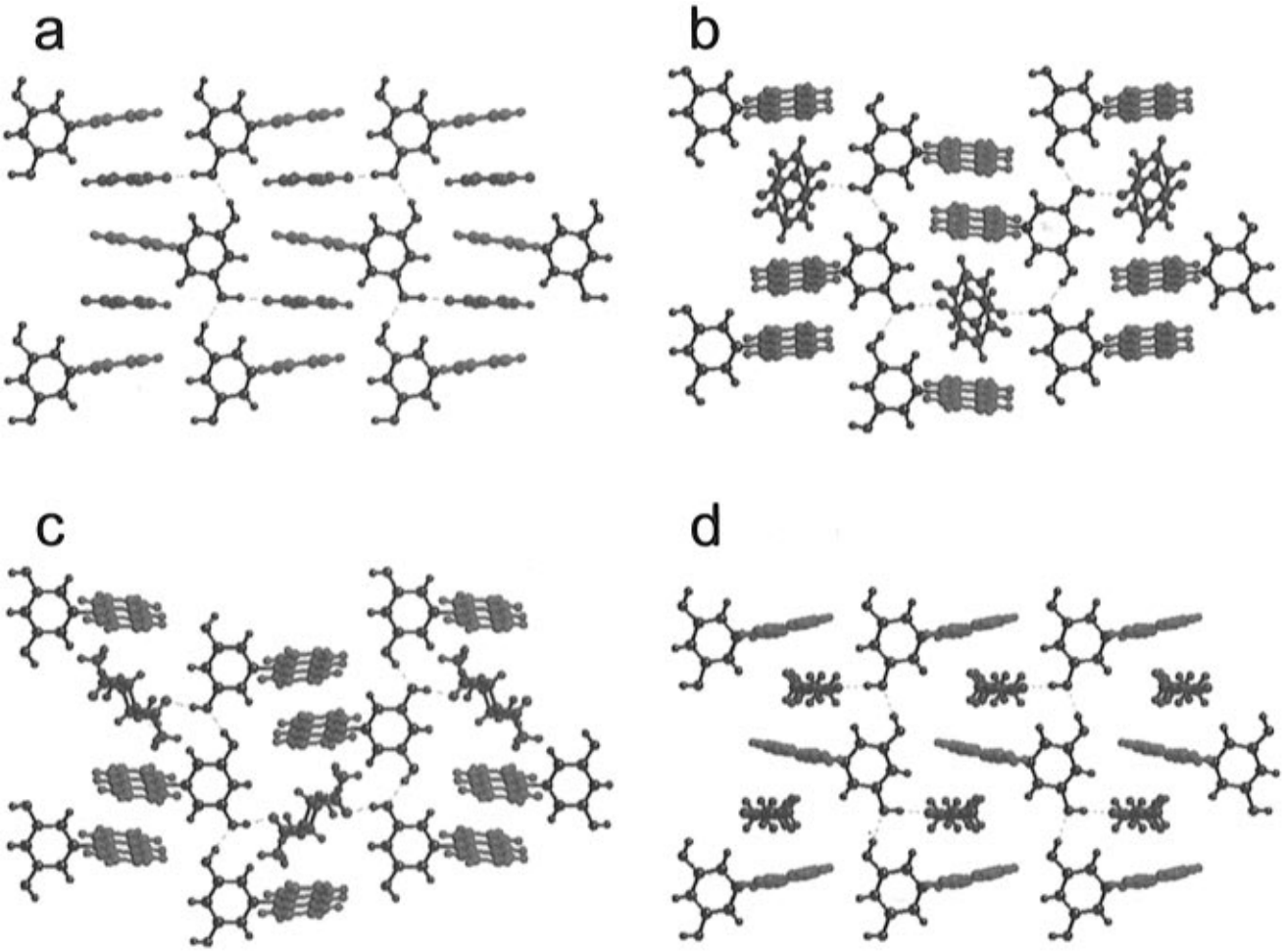

Figure 2. Side views of a molecular sheet for adducts **1·3c** (a), **1·5a** (b), **1·8b** (c), and **1·9c** (d). The colors have the same meanings as in Figure 1.

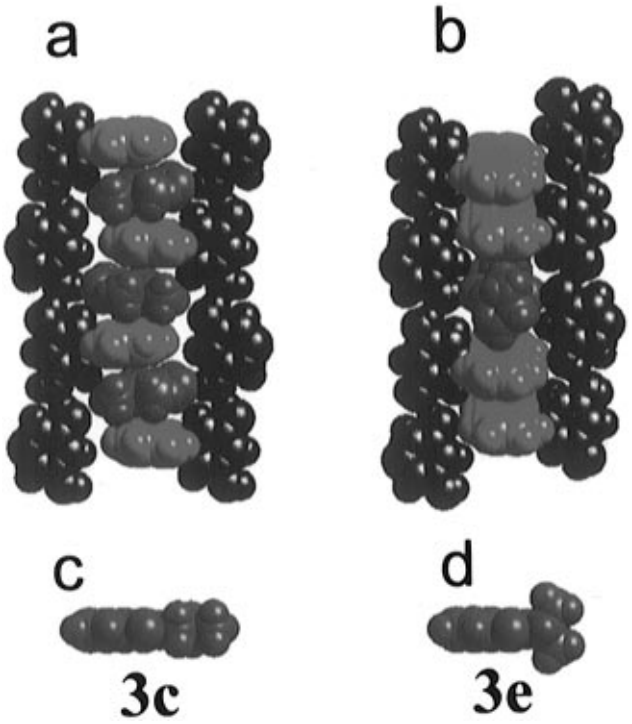

Figure 3. Space-filling molecular models for the crystal structures of adducts **1·5b** (a) and **1·10** (b), propyl benzoate (**3c**) (c), and isopropyl benzoate (**3e**) with its branched alkyl group in a *vertical* conformation (d). The colors have the same meanings as in Figure 1.

Excimers and exciplexes in solutions are usually in rapid and dynamic equilibria with their components. The present results

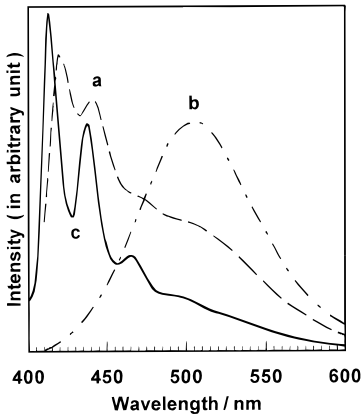

Figure 4. Fluorescence spectra for adducts **1·3c** (a), **1·8b** (b), and **1·9c** (c) dispersed in KBr at 25 °C.

indicate that *stable* monomer and excimer fluorescent states as well as nonfluorescent charge-transfer states can be selectively constructed by the solid-state dilution, dimerization, and complexation of the fluorophores on the self-assembling 1D chains. It should be noted that anthracene emits excimer fluorescence neither in the solid state nor in solution at room temperature.[10] The excimer state of it is accessible only by an in-situ photodissociation of dianthracene, i.e., anthracene photodimer, at 77 K in KBr[11] or a methylcyclohexane glass.[12] In marked contrast, the present pattern-*d* adducts with an enforced excimer structure *exclusively* emit excimer fluorescence at room temperature.

Selectivity in Competitive Cocrystallization. The change in the cavity sizes is another important consequence of the

Table 2. Competitive Cocrystallization of Host **1**

entry	guest A	guest B	A/**1**	B/**1**	(A + B)/**1**	A/B[a]
1	**3a**	**8b**	~1	≤0.05	1	≥20
2	**9b**	**9a**	~1	<0.01	1	vl
3	**10**	**9b**	~1	≤0.04	1	≥30
4	**8a**	**8b**	0.4	0.6	1	0.7
5	**8b**	**8c**	0.3	0.7	1	0.4
6	**8c**	**8d**	0.7	0.3	1	2
7	**8b**	**8e**	0.3	0.7	1	0.4
8	**8e**	**8f**	0.4	0.6	1	0.7
9	**9f**	**9g**	0.3	0.7	1	0.4
10	**9g**	**9c**	0.4	0.6	1	0.7
11	**9b**	**9c**	0.2	0.8	1	0.2
12	**9c**	**9d**	0.8	0.2	1	4
13	**3a**	**3b**	0.8	0.2	1	4
14	**3b**	**3c**	0.6	0.4	1	1.5
15	**3c**	**3d**	0.65	0.35	1	2
16	**3a**	**3e**	~1	≤0.04	1	≥30
17	**3a**	**3f**	~1	≤0.03	1	≥30
18	**9b**	**9h**	~1	≤0.03	1	≥30
19	**9c**	**9h**	~1	< 0.02	1	vl
20	**9c**	**9i**	~1	0	1	vl
21	**4b**	**4c**	~1	0	1	vl

[a] vl = very large.

switch from the 2D network to self-assembling 1D chains. The width and depth of a cavity are reflected on the intercolumn (*Ic*−*c*) and intersheet (*Is*−*s*) distances, which are roughly similar for the 1D and the 2D systems.[8] It is in the effective height or thickness of a cavity that the monoanthracenyl 2D (**2**) and dianthracenyl 1D (**1** or **11**) systems differ.

Competitive cocrystallization of host **1** from an equimolar mixture of two guests, A and B, afforded ternary adducts; molar ratios therein, A/**1** and B/**1**, are shown in Table 2. The total guest/host ratios are always (A + B)/**1** = 1. The competition between pattern-*m* guests vs pattern-*d* guests is remarkably in favor of the bulkier guests (entries 1−3), reflecting better crystal packing therewith. Entries 4−6 (alkyl acetates, i.e., alkoxy methyl ketones; 2 < 3 < 4 > 5), 7 and 8 (ethyl alkanecarboxylates, i.e., alkyl ethoxy ketones; 1 < 2 < 3), 9 and 10 (alkyl propyl ketones; 1 < 2 < 3), and 11 and 12 together with 2 (symmetrical dialkyl ketones; 1 < 2 < 3 > 4) are concerned with chain-length selectivities. The affinities change with respect to the chain lengths of the alkyl or alkoxy moieties in the order shown in parentheses. The optimal chain length of 3 for symmetrical dialkyl ketones may be compared with that of 4 in the competitive cocrystallization with 2D host **2**.[4b]

Entries 13−17 show a striking selectivity among alkyl benzoates, i.e., alkoxy phenyl ketones. The affinities with respect to the alkyl groups decrease in the order methyl > ethyl > propyl > butyl ≫ isopropyl ≈ isobutyl, the highest/lowest selectivity being methyl/isopropyl ≈ methyl/isobutyl ≥ 30 (entries 16 and 17). This is in dramatic contrast to the selectivity in the related cocrystallization with host **2**, where the affinities *increase* in the same order, i.e., methyl < ethyl < propyl < isobutyl, with the highest/lowest selectivity of isobutyl/methyl ≥ 70.[4b] Thus, the change in the network dimensionality (1D vs 2D) leads to a drastic (≥2000-fold) change in the methyl/isobutyl selectivities.

The lowest affinities of isopropyl and isobutyl benzoates (**3e** and **3f**) suggest that branching is the governing factor. A space-filling molecular model for isopropyl benzoate (**3e**) with its alkyl group in the *thickest* or *vertical* conformation is shown in Figure 3d, together with that for propyl benzoate (**3c**) in Figure 3c. A comparison of these with Figure 3a suggests that the branched alkyl group in guest **3e** or **3f** is too thick to be accommodated in the pattern-*m* cavity with an effective height or thickness of ~3.7 Å, although a linear alkyl chain is accommodatable therein. In marked contrast, the branched alkyl groups are cavity-filling and hence affinity-enhancing when incorporated in a larger or thicker cavity provided by 2D host **2** (Figure III, Supporting Information).

Interestingly, recrystallization of host **1** from isopropyl benzoate (**3e**) only affords a 1:2 adduct, **1**·2(**3e**),[13] in which each OH group of the host is hydrogen-bonded to the guest (structure **12** in Chart 1); there is no host−host hydrogen bond and hence no hydrogen-bonded network (the crystal packing mode is shown in Figure IV of the Supporting Information). In marked contrast, propyl benzoate (**3c**) readily affords 1:1 cocrystal **1**·**3c** with lattice pattern *m* (Figure 2a). If it were not for self-assembly (self-intercalation), a single 1D chain of host **1** could accommodate guests **3e** and **3f** in a similar manner as host **2**. This is not the case, however. Thus, the formation of hydrogen-bonded 1D chains, self-assembly thereof, and binding of appropriate guests in the resulting cavities must be highly cooperative.

The branching effect turns out to be a general phenomenon. Entries 18−21 are concerned with the competitions between linear-alkyl (ethyl or propyl) vs branched-alkyl (isopropyl or isobutyl) groups in the binding of ketones. In every case, a remarkably high preference (~100:0) for the linear alkyl groups is observed.

Apohost and Its Guest-Binding Properties. Included volatile guests such as ethyl acetate can be removed to give a polycrystalline apohost,[14] whose powder X-ray diffractions are shown in Figure Va (Supporting Information). When dipped in methyl benzoate, ethyl acetate, or 4-heptanone at ≤ 3 °C,[15] the apohost readily binds one molecule of the guest in minutes. These guests can be bound readily also under the solid−gas conditions[4b] at 25 °C. The resulting adducts **1**·**3a**, **1**·**8b**, and **1**·**9c** show identical powder X-ray diffractions as well as fluorescence spectra as the corresponding single crystals obtained by direct recrystallization. Hydrocarbon guests such as hexane, benzene, and alkylbenzenes as either liquids or gases can be bound in a similar manner. Guest exchange also takes place. For example, ethyl acetate adduct **1**·**8b** dipped in methyl benzoate (**1**·**3a**) or 4-heptanone (**1**·**9c**) at −23 °C[15] affords guest-exchanged adduct **1**·**3a** or **1**·**9c** in hours, whose powder X-ray diffractions and fluorescence spectra are again identical with those of the corresponding single-crystalline sample. The powder diffractions of adducts **1**·**9c** and **1**·**3a** obtained in three different ways, i.e., recrystallization, guest-binding to apohost **1**, and guest-exchange using adduct **1**·**8b**, are shown in Figure V (b−g) in the Supporting Information. Reorganization of 1D chains from lattice pattern *d* (for **1**·**8b**) to pattern *m* (for **1**·**3a** or **1**·**9c**) must have taken place during the guest exchange. Thus, the characteristic guest-binding properties of the 2D apohost **2**[4b] are also characteristic of the 1D apohost **1**, although, as noted above, the guest-binding cavities in the latter must be significantly more compact than those in the former.

Concluding Remarks

This work may be summarized as follows: (1) Lateral alignment of the present 1D chains actually involves self-

(13) Formula, $C_{40}H_{38}O_6$; formula weight, 614.74; crystal system, triclinic; space group, *P*-1 (no. 2); color, colorless; a = 9.084(1) Å, b = 21.342(3) Å, c = 9.048(3) Å, α = 98.19(2)°, β = 105.90(2)°, γ = 90.94(1)°, V = 1667.1(6) Å^3, Z = 2, d = 1.225, no. of uniq rflc = 7671, no. of rflc used = 2512, GOF = 1.18, R = 0.040.

(14) Apohost **1** dispersed in KBr shows a featureless emission at 446 nm when irradiated at 408 nm.

(15) The choice of low temperatures is to minimize dissolution of the host and its adducts. Nevertheless, exchange may involve dissolution and recrystallization; the mechanism of guest-exchange under the solid−liquid conditions has not been established. For related work, see: (a) Wang, X.; Simard, M.; Wuest, J. D. *J. Am. Chem. Soc.* **1994**, *116*, 12119−12120 (footnote 16). (b) Reference 4b (footnote 20).

intercalation of the orthogonal anthracene rings. (2) Thus, the rigid and porous 2D network of triad **2** can be replaced by a more tightly packed and hence less porous pseudo-2D network of diad **1**. (3) The packing is governed by the hydrogen-bonded network and manipulated by guest molecules. The present approach provides a *general* strategy for designing aromatic stacks and columns, whose photophysical properties are guest-controllable. (4) The thickness of a cavity is also strictly controlled by the hydrogen-bonded network. This results in a novel thickness selectivity in the guest binding, showing a remarkable discrimination of linear vs branched alkyl groups. (5) As a summary, the present work points to the importance and utility of functional self-assembly of designed interaction networks.

Experimental Section

Compound **1** was prepared (in a total yield of 44%) in a manner similar to that of compound **2**,[4b] i.e., with 9-bromoanthracene in place of 9,10-dibromoanthracene as the starting material. The crystal structure determinations and recrystallization, guest-binding, and guest-exchange studies were carried out also in a manner similar to those of the 2D (**2**) systems. Details of experimental procedures are shown in the Supporting Information.

Acknowledgment. This work was supported by grants-in-aid from the Ministry of Education, Science, and Culture of the Japanese Government. We are also grateful to Rigaku Co. Ltd. and Professors M. Ohta and S. Matsuya (Faculty of Dentistry, Kyushu University) for the measurements of powder X-ray diffractions.

Supporting Information Available: Table 1 giving crystal parameters, tables of crystal structural data with thermal ellipsoid figures including atomic coordinates, B_{iso}/B_{eq} and occupancy, anisotropic displacement parameters, bond lengths, bond angles, torsion angles, and nonbonded contacts out to 3.60 Å for adducts **1·3a**, **1·3c**, **1·2**(**3e**), **1·4a**, **1·5a**, **1·5b**, **1·6**, **1·7**, **1·8a**, **1·8b**, **1·9a**, **1·9b**, **1·9c**, **1·9e**, **1·9g**, and **1·10**, Figures I and II showing side views of a molecular sheet in adducts **1·3a**, **1·4a**, **1·6**, **1·7**, **1·8a**, **1·9a**, **1·9b**, **1·9e**, and **1·9g**, Figure III showing the crystal structure of adduct **2**·2(**3f**) in stereo, Figure IV showing the crystal packing mode for adduct **1**·2(**3e**), Figure V showing powder X-ray diffractions for apohost **1** and adducts **1·9c** and **1·3a**, and text giving experimental details (170 pages). See any current masthead page for ordering and Internet access instructions.

JA960292X